

Geophysical Research Letters

RESEARCH LETTER

10.1029/2020GL091790

Key Points:

- Totten's grounding line is steady and close to present-day only for current ocean temperatures and retreats for small temperature increases
- Ocean variability of various amplitudes can reduce discharge and cause centennial scale delays in grounding line migration
- Forcing variability needs to be taken into account in ice sheet model simulations of future climate change

Supporting Information:

Supporting Information may be found in the online version of this article.

Correspondence to:

F. S. McCormack,
felicity.mccormack@monash.edu







Citation:

McCormack, F. S., Roberts, J. L., Gwyther, D. E., Morlighem, M., Pelle, T., & Galton-Fenzi, B. K. (2021). The impact of variable ocean temperatures on Totten Glacier stability and discharge. *Geophysical Research Letters*, 48, e2020GL091790. <https://doi.org/10.1029/2020GL091790>

Received 23 NOV 2020

Accepted 24 APR 2021

The Impact of Variable Ocean Temperatures on Totten Glacier Stability and Discharge

F. S. McCormack^{1,2} , J. L. Roberts^{3,4} , D. E. Gwyther⁵ , M. Morlighem⁶ , T. Pelle⁶ , and B. K. Galton-Fenzi^{3,4} 

¹School of Earth, Atmosphere & Environment, Monash University, Clayton, VIC, Australia, ²Institute for Marine and Antarctic Studies, University of Tasmania, Battery Point, TAS, Australia, ³Australian Antarctic Division, Kingston, TAS, Australia, ⁴Australian Antarctic Program Partnership, Institute for Marine and Antarctic Studies, University of Tasmania, Battery Point, TAS, Australia, ⁵Centre for Applications in Natural Resource Mathematics, School of Mathematics and Physics, University of Queensland, St Lucia, QLD, Australia, ⁶Department of Earth System Science, University of California, Irvine, CA, USA

Abstract A major uncertainty in Antarctica's contribution to future sea-level rise is the ice sheet response timescales to ocean warming. Totten Glacier drains a region containing 3.9 m global sea level equivalent and has been losing mass over recent decades. We use an ice sheet model coupled to an ice-shelf cavity combined ocean box and plume model to investigate Totten's response to variable ocean forcing. Totten's grounding line is stable for a limited range of ocean temperatures near current observations (i.e., -0.95°C to -0.75°C), with topography influencing the discharge periodicity. For increases of $\geq 0.2^{\circ}\text{C}$ in temperatures beyond this range, grounding line retreat occurs. Variable ocean forcing can reduce retreat relative to constant forcing, and different variability amplitudes can cause centennial-scale delays in retreat through interactions with topography. Our results highlight the need for long-term ocean state observations and to include forcing variability in ice sheet model simulations of future change.

Plain Language Summary Antarctica's contribution to future sea-level rise is dominated by uncertainties in how the ice sheet will respond to ocean warming. Totten Glacier, East Antarctica, currently contributes to sea-level rise and is the major outlet glacier in a region with potential to significantly raise sea levels. We use an ice sheet model coupled to a combined box and plume ocean model to investigate how variability in ocean temperatures can impact ice mass loss in this region. For scenarios of ocean temperatures that are near observed, the grounding line position is close to its present-day location. In these scenarios, interactions between the ice shelf and topography are important in controlling the timing between peak ice shelf melting and peak mass changes. For small increases in background ocean temperature, we see grounding line retreat. In these scenarios, variability in ocean temperatures can reduce ice flux across the grounding line compared with when the ocean temperature is constant. Certain amplitudes of variability can delay grounding line retreat by centuries through interactions with the topography. This highlights the need for long-term ocean observations in this region and to include ocean variability in ice sheet model simulations of future change.

1. Introduction

The Antarctic Ice Sheet has been losing mass at an accelerating rate over recent decades (Smith et al., 2020). Most of this mass loss can be attributed to ocean-driven ice shelf thinning that weakens the buttressing effect acting on grounded ice and accelerates ice discharge (Gudmundsson et al., 2019). Antarctica's contribution to sea-level rise over the coming century is likely to accelerate (Seroussi et al., 2020), particularly as a result of ice loss from marine-based sectors that are susceptible to instability (Schoof, 2007; Weertman, 1974). However, the magnitude and timing of future Antarctic ice mass loss in response to climate warming constitute the largest source of uncertainty in projections of sea-level rise (Oppenheimer et al., 2019). Contributing to this uncertainty is the impact of climate variability on ice sheet mass loss, the upper bounds of which are generally poorly constrained (Robel et al., 2019).

Totten Glacier is the primary outlet glacier of the Aurora Basin (AB)—draining a region containing 3.9 m of global sea level equivalent (Morlighem et al., 2020)—and is likely to be the largest East Antarctic contributor to sea-level rise over the coming century (Pelle et al., 2020). Similar to studies from the marine sectors of West Antarctica (e.g., Jacobs et al., 1996, 2011, 2013; Jenkins et al., 2010, 2018), recent thinning of the Totten Ice Shelf (TIS; Adusumilli et al., 2020; Flament & Rémy, 2012) is likely to be driven by increasing intrusion of warm Circumpolar Deep Water (CDW; Rintoul et al., 2016; Silvano et al., 2017). A recent modeling study shows that under ocean state conditions similar to present-day, Totten grounding line retreat occurs, with faster retreat for increasing ocean temperatures (Sun et al., 2016). Should sustained ocean warming cause retreat into the main tributary feeding the TIS, where the bed slopes downwards into the interior of the continent, Totten is a potential candidate for instability (Pelle et al., 2020). This could lead to substantial grounding line retreat, as indicated by paleo evidence of past grounding line locations in the interior of the AB catchment (Aitken et al., 2016).

The TIS also has a highly variable thickness record, fluctuating by 2 ± 7.5 m per decade (Paolo et al., 2015). This may be linked to variability in the supply of CDW to the ice shelf cavity resulting from wind-driven upwelling changes (Greene et al., 2017). Recent modeling evidence from West Antarctica suggests that when coupled with mean state changes, variability can alternately increase (Holland et al., 2019) or delay (Hoffman et al., 2019) ice mass loss and grounding line retreat. However, ocean variability in the Totten region is poorly constrained due to a paucity of long-term climate and ocean state measurements in this region. Furthermore, the impact of variability in ocean thermal forcing on the long-term dynamics and stability of Totten is unknown.

Here, we investigate Totten's response to a range of ocean thermal forcings of different background temperatures and amplitudes of variability. We use the finite-element Ice-sheet and Sea-level System Model (ISSM; Larour et al., 2012) coupled to the Potsdam Ice-shelf Cavity model combined with a Plume model (PICOP; Lazeroms et al., 2018; Pelle et al., 2019; Reese et al., 2018) to parameterize ocean-driven ice shelf basal melt rates. We consider the role of topographic pinning points in modulating the impact of variable ocean thermal forcing, with the aim of better understanding grounding line stability and dynamics in this system.

2. Data and Methods

2.1. Ice Sheet Model

We use ISSM to run simulations of the AB catchment (Figure 1a). The horizontal mesh comprises 114,915 anisotropic, triangular elements, ranging from a refined mesh of 1 km resolution in the grounding zone of the TIS and Moscow University Ice Shelf (MUIS) to approximately 20 km in the interior of the basin. The model uses the shelfy-stream approximation (SSA; MacAyeal, 1989) to the Stokes equations. The ice shelf front position is held constant throughout each experiment.

The bed topography, initial grounding line, and ice thickness are taken from BedMachine Antarctica (Morlighem et al., 2020). Surface temperature and mass balance (SMB) are from the Regional Atmospheric Climate Model RACMO2.3 (Lenaerts et al., 2012). Surface velocities are from Rignot et al. (2011, 2017). The basal friction is calculated using a linear viscous relation and the spatially varying basal friction coefficient is estimated using inverse methods (Morlighem et al., 2013). Both the basal friction and ice stiffness coefficients remain fixed throughout the simulations (Figure S1). More details on the model and initialization are provided in supporting information S1.

We use PICOP (Pelle et al., 2019) to estimate ice shelf melt rates. PICOP builds on PICO (Reese et al., 2018), parameterizing both the sub-shelf vertical overturning circulation and the impact of buoyant meltwater plumes (Lazeroms et al., 2018) on ocean-driven melt rates. The input far-field ocean salinity and temperature fields represent the average salinity and temperature in the lowest ocean layer of the continental shelf region. PICOP estimates of basal melt have been shown to agree well with satellite-derived estimates beneath the TIS (Pelle et al., 2019). We apply ice shelf melt rates only to entirely floating model elements to avoid overestimating total ice shelf basal melt and, therefore, introducing biases toward more retreat, as shown in Seroussi and Morlighem (2018).

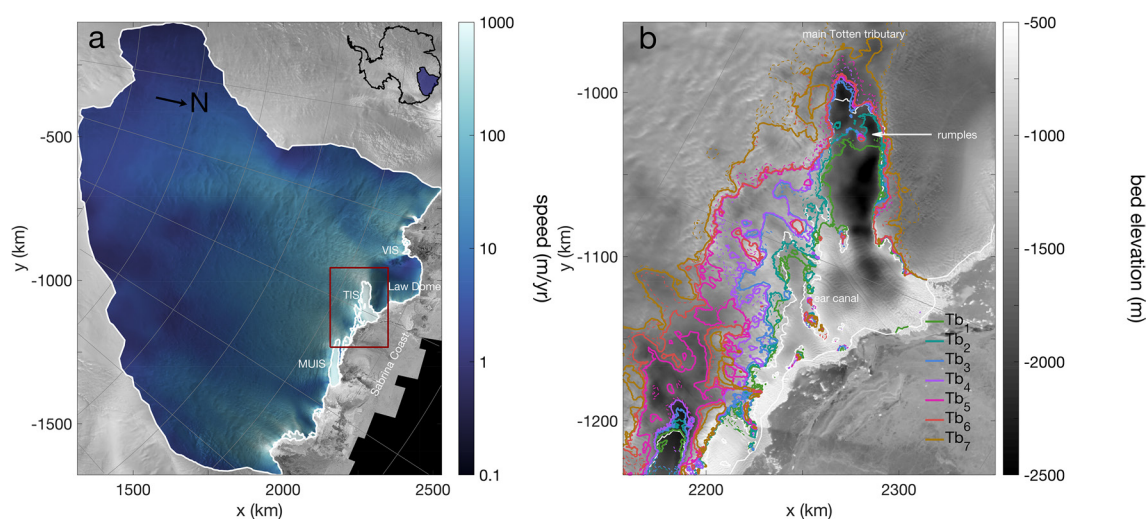


Figure 1. (a) Aurora Basin (AB) model domain, showing the locations named in the text, including the Totten Ice Shelf (TIS), Moscow University Ice Shelf (MUIS), and Vanderford Ice Shelf (VIS). The observed ice surface speed (logarithmic scale; m/yr), and ice front, and initial grounding line position (white contour) are shown. In both panels, the background imagery is from Jezek (2013). The region within the red box in (a) is enlarged in (b), where the gray shading is the BedMachine Antarctica bed elevation (m) (Morlighem et al., 2020). The thin, dashed contours are the final grounding line positions for the constant forcing cases (Section 3.1); the thick, solid contours are the final grounding line positions for the VA5 variability cases (Section 3.2). The x - and y -axes are polar stereographic eastings and northings (km), respectively, with 71°S as the latitude of true scale and 0°E as the reference longitude.

2.2. Experiments

We consider the ice sheet response to background ocean temperatures (Tb) increasing from $Tb_1 = -1.15^\circ\text{C}$ to $Tb_7 = 0.05^\circ\text{C}$ in 0.2°C increments. The first set of experiments applies each of these background temperatures as temporally constant ocean thermal forcing, leading to seven simulations. The salinity is fixed at 34.73 on the Practical Salinity Scale PSS-78 following Reese et al. (2018), which is broadly consistent with far-field (off-continental shelf) observations (Schmidtke et al., 2014).

The second set of experiments applies a time-varying temperature anomaly to each of the constant background temperatures Tb_1 – Tb_7 . While ship-based observations confirm the presence of CDW from the continental shelf to the TIS front (Nitsche et al., 2017; Rintoul et al., 2016; Silvano et al., 2017; Wakatsuchi et al., 1994; Williams et al., 2011), we do not have the repeat seasonal and multiyear observations to establish bounds on interannual to decadal ocean variability in this region. We generate our anomaly time series based on output from a 200 years numerical ocean model of the Sabrina Coast sector (Gwyther et al., 2018). The boundary conditions consist of a repeating invariant annual cycle of forcing. Hence, in this ocean model simulation, variability with periods greater than 1 year results from ocean dynamics that are generated internally (intrinsic ocean variability) as a response to stochastic forcing, but not from multiyear boundary conditions or longer-period atmospheric variability. Details of the ocean model simulation are further discussed in supporting information S2.

We first calculate a normalized autoregressive model of second-order AR(2) (von Storch & Zwiers, 1999) that fits the area-averaged sub-shelf (top layer) temperature anomalies of the ROMS simulation. We then use the coefficients estimated from this fitting to filter a white noise time series, generating a new temperature anomaly time series that is statistically consistent with that of the original ocean model simulation. Extending the length of the white noise record in this way allows us to perform ice sheet model simulations for time periods longer than the output of the original ocean model simulation.

The resulting temperature anomaly time series is based on an ocean model simulation that has a lower amplitude of variability than observed (Gwyther et al., 2018) and requires scaling to minimize this mismatch. We generate forcing time series VA1–VA10 by multiplying the original time series by factors 1–10 (Figure S2). Here, VA5 is the variability amplitude scaling nominally representative of the observations; the Tb_3 background temperature with variability amplitude VA5 produces melt rates and discharge most consistent

with observations (Figure S3). The VA1–VA10 temperature time series have rms amplitudes ranging from 0.2 to two times the VA5 simulation.

The same VA1–VA10 time series are applied to each background temperature, resulting in a total of 70 simulations with variable ocean forcing. Each of the constant and variable forcing experiments are run for 500 years with a model time step of 5 days. The velocities, geometry (thickness and surface elevation), and grounding line are updated at each time step. The first ~100 years of the simulation time constitutes a period of ice sheet adjustment to changed boundary conditions (the time taken to traverse the length of the TIS using observed velocity fields is ~127 years); beyond this the dynamics are internally consistent. Hence, in what follows, we present and analyze the final 400 years of the simulations. We note that the periods of variability captured in our AR(2) time series might not directly correspond to the dominant periods forcing this ice shelf given the ~127 years ice shelf transit time. However, the focus of this study is the relatively short (interannual to multidecadal; see Section 4.3) periods of variability in the ice sheet response.

3. Results

3.1. Constant Temperature Forcing

The final grounding line positions for each of the constant temperature forcing cases are shown in Figure 1b. The final grounding line position is steady only for Tb_2 ; for Tb_1 the grounding line advances and for Tb_3 – Tb_7 the grounding line retreats over the 500 years simulations. Similar to Schlegel et al. (2018), the rate of grounding line migration for our simulations is not constant, but varies temporally and spatially depending on the local topography that influences the retreat and advance pathways and buttressing (Movie S1).

For Tb_2 , the final grounding line at the southern end of the TIS—the main tributary through which the majority of the mass flux originates—is advanced on a plane of relatively higher bathymetry (Greenbaum et al., 2015) and rumples (Figure 1b) that have been previously documented (Roberts et al., 2017). Along the eastern flank of the TIS, the final grounding line is generally within 5 km of the observed position. Grounding over rumples also occurs between the ice-ocean front and the “ear canal,” west of the deep bathymetric trough that provides a pathway for potential incursion of CDW (Greenbaum et al., 2015).

For Tb_3 – Tb_7 , the grounding line first retreats through the eastern flank of the TIS, with faster retreat for higher temperatures. For Tb_3 and Tb_4 , the grounding line also retreats approximately 6.5 km into the main Totten tributary relative to the Rignot et al. (2017) grounding line, stabilizing on a prograde slope in a region of depressed bed topography (Figure 1b) where the TIS is thickest (Morlighem et al., 2020). The MUIS and TIS merge within 280 years of the simulation for Tb_6 . Finally, for Tb_7 , widespread and rapid retreat results in one continuous ice shelf in this region, and melt rates are sufficiently high to drive retreat over the prograde bed slope at the southern end of the TIS into the AB.

TIS area-averaged melt rate and discharge (flux across the Totten grounding line) are shown in Figure 2. Tb_1 shows a reduction in discharge corresponding to a reduced TIS area (fixed calving front, but advanced grounding line). For all other experiments, fluctuations in discharge are related to grounding line migration as well as variations in ice-shelf thickness and buttressing.

3.2. Variable Temperature Forcing

The final grounding line positions for the variable forcing cases with amplitude VA5 are shown in Figure 1b (Figure S4 shows the grounding line positions for all amplitudes). There is reasonable agreement between the final grounding lines for the constant and variable forcing cases, particularly for lower background temperatures. However, for Tb_6 and Tb_7 , the grounding lines for the constant forcing simulations are generally retreated compared to the variable simulations. For Tb_2 and Tb_3 , the final grounding line positions are not fixed, fluctuating by up to 5 km/decade in some regions. This is particularly the case where there is complex topography, such as near the rumples at the southern end of the TIS and along the eastern flank.

The extent of grounding line retreat or advance is not always a clear function of the variability amplitude (Figure S4), and neither are the timescales of grounding line retreat. For example, for Tb_7 , the grounding line retreat is slowest for the VA7 amplitude between years 115 and 370. After 370 years, the grounding line

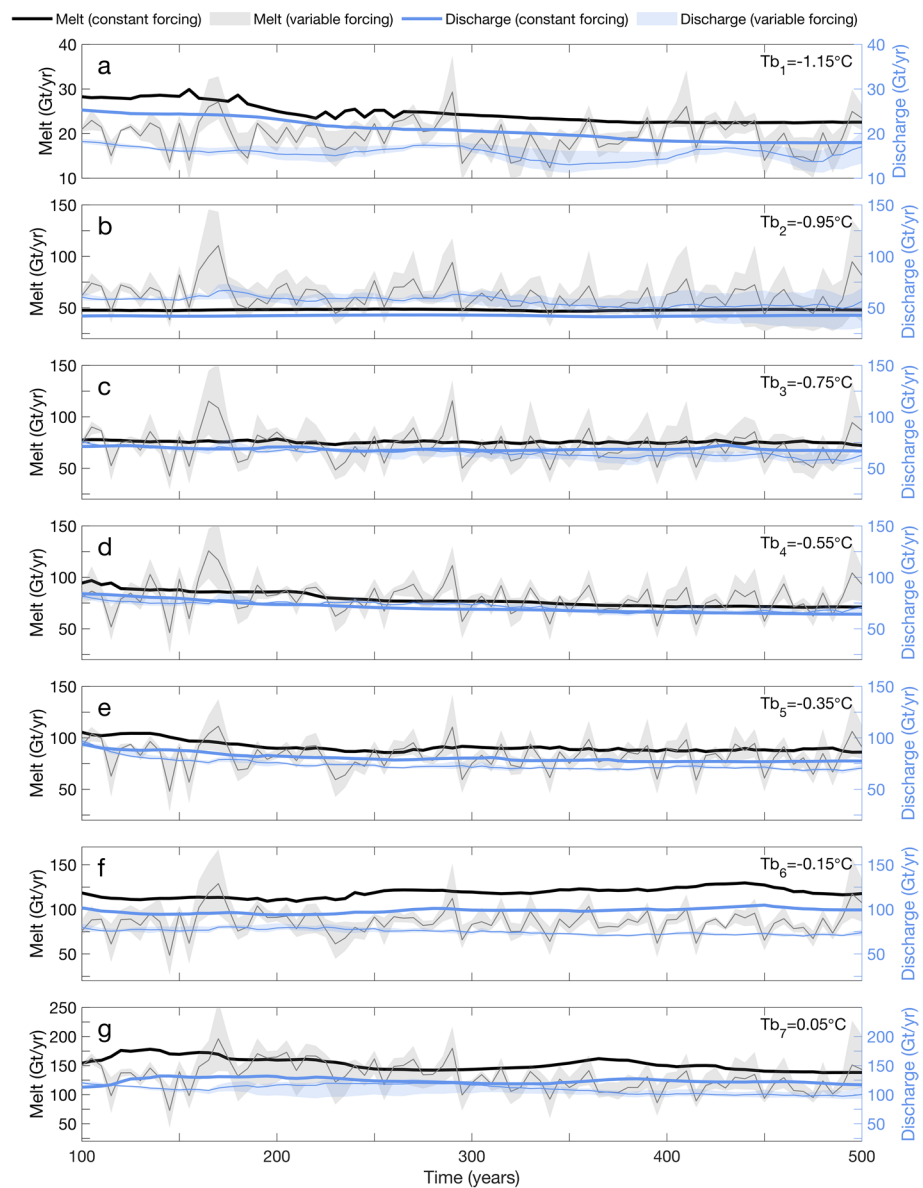


Figure 2. Left y-axis for each panel is TIS area-averaged melt rate (Gt/year) and the right y-axis is discharged into TIS (positive from grounded to floating ice; Gt/year) for (a) Tb_1 – (g) Tb_7 . The bold lines are values from the constant thermal forcing experiments. The shaded areas represent the range of scenarios for the variable thermal forcing simulations and the thin solid line is the median value of this range for the given background temperature. Note the different y-axis scales. The temperature value reported next to each experiment name is the far-field mean ocean thermal forcing.

rapidly retreats and the final position is close to those of the remaining experiments. Similar retreat behavior is observed for certain variability amplitudes in the Tb_2 , Tb_3 , Tb_5 , and Tb_6 cases.

The melt rates and discharge generally increase for increasing background temperatures (Figure 2). The Tb_2 and Tb_3 results show the largest spread in melt rates and discharge across the different variability amplitudes; for Tb_2 , the final discharge rates vary by almost a factor of 2.5 between the VA1 and VA10 cases. In scenarios of grounding line advance and retreat (i.e., Tb_1 and Tb_5 – Tb_7), variability leads to lower mean melt rates compared with the constant forcing cases, with subsequent reductions in discharge.

4. Discussion

4.1. Grounding Line Stability

Our simulations over a range of background ocean temperatures collectively encompass scenarios of grounding line advance, stability, and retreat (here, we use “stable” to indicate grounding line fluctuations of less than 5 km). Under constant and variable thermal forcing, the grounding line is stable only for Tb_2 . For Tb_3 , the grounding line retreats continuously in the latter half of the constant forcing scenario, which is consistent with the findings of Sun et al. (2016); for VA5, the grounding line retreats early, then advances to a similar final position to the constant case. Given that the Tb_3 far-field ocean temperature is closest to observed (Reese et al., 2018; Schmidtke et al., 2014), this indicates that ocean variability could play a role in stabilizing grounding line migration under present-day ocean forcing. The southern-most portion of the grounding line in the Tb_3 simulation is closest to its observed location during periods of contact between the TIS and the southern rumple (Section 4.3), suggesting a controlling influence of topography on grounding line stability under present-day forcing, as previously hypothesized (Roberts et al., 2017).

For Tb_1 , grounding line advance occurs and the final locations from all experiments except VA1 and VA2 are within 3.5 km of each other (Figure S4). Small increases in the background temperature beyond Tb_2 lead to grounding line retreat compared with the observations. As previously reported (Pelle et al., 2020; Sun et al., 2016), grounding line retreat occurs first and is most extensive through the eastern flank, although retreat here has a limited impact on sea-level rise (Pelle et al., 2020). Grounding line retreat onto the retrograde-sloping bed of the AB—where marine ice sheet instability might arise—occurs only for Tb_7 under both constant and variable forcing. The addition of variability in the retreat scenarios tends to reduce grounding line migration.

There are a number of limitations in our modeling approach that impact the estimates of grounding line migration, including: (1) PICOP does not capture coupled ice-ocean processes that impact the magnitude of basal melting and consequent buttressing (Seroussi et al., 2017; Snow et al., 2017); (2) the use of SSA, which can lead to less grounding line migration and mass loss than the Stokes equations (Yu et al., 2018); and (3) we use the Budd et al. (1979) friction law that has been shown to produce more extensive grounding line migration under warming scenarios than other friction laws (Yu et al., 2018). It is possible that (2) and (3) partially compensate for each other; nevertheless, future work should explore the effects of these on ice mass loss estimates from the AB.

4.2. Ice Sheet Dynamics

The impact of variability on ice sheet dynamics depends on the complex interplay between the mean ocean thermal forcing, the variability amplitude, and the ice sheet response to these forcings, modulated by interactions with topography.

For Tb_1 , Tb_3 , and Tb_5 – Tb_7 the ice sheet responds differently to variable forcing than to constant forcing, with a reduction in grounding line migration and discharge under variable forcing relative to constant forcing (Figures 1b and 2). This may be linked to the fact that the TIS is thicker on average under variable forcing than constant forcing for Tb_1 , Tb_3 , and Tb_5 – Tb_7 , which implies increased buttressing and an effective cap on discharge in the variable forcing cases (Figures 2 and S5). Hoffman et al. (2019) report a similar result, which they demonstrate arises from nonlinear dynamics in the ice sheet response to variable forcing, whereby the system is more sensitive to increases in ice thickness during periods of lower average melt than to ice shelf thinning under heightened melt rates. It is possible that a similar nonlinear dynamic response is operating in this study, particularly given that a nonlinear dynamic response to ice shelf thinning is also evident in Reese et al. (2018) (supporting information). There is also a reduction in grounding line retreat for Tb_4 under variable forcing compared with constant forcing. However, the discharge under variable forcing for Tb_4 is slightly higher in the final 100 years of simulation, reflecting generally higher melt rates as the ice shelf geometry adjusts to ongoing grounding line migration.

The same response is not seen for Tb_2 under variable forcing. In this case, there is a greater spread between the final grounding line positions through the main Totten tributary for Tb_2 than for any other background temperature (Figure S4), which leads to a large spread of discharge estimates for the VA1–VA10 simulations

(Figure 2). In eight of the 10 variable forcing simulations, the grounding lines are retreated compared with the constant case (which is advanced compared to observed) and located in regions of deeper bathymetry and/or faster ice flow, which leads to greater discharge. It is possible that Tb_2 , which is only slightly cooler than observed, is close to a threshold temperature for this system, such that small perturbations in ocean temperature above -0.95°C can lead to relatively large differences in grounding line locations and discharge. This warrants further investigation, particularly into the observations that are needed to establish the mean ocean state and stability thresholds, and the role of fine-scale topography in influencing grounding line migration in the main Totten tributary.

The extent and timescales of grounding line migration do not necessarily correlate with the variability amplitude. For example, in the VA7 simulation for Tb_7 , the grounding line retreat is delayed between years 115 and 370 compared with all other variability amplitude cases (Figure S6) due to stabilization along a ridge at the south-eastern end of the TIS. For Tb_2 , the VA6 simulation has the most retreated grounding line of any of the variability amplitudes along parts of the eastern flank (Figure S4). Similar anomalous behavior for different variability amplitudes occurs for each of the background temperatures (Figure S4). These results suggest that specific forcing frequencies may be amplified or attenuated under certain amplitudes of ocean variability (Figure S7), modifying the ice sheet dynamics and response timescales. This may also explain the lack of a consistent relationship between variability amplitude and TIS thickness and discharge for all background temperatures (Figure S5). This result complicates the interpretation of observations as it indicates that neither the amplitude of variability nor the background temperature magnitude is a sufficient predictor of the timing of the ice sheet response or even the phase of the response over the timescale of current observations.

4.3. Discharge Periodicity

Finally, we investigate the impact of ocean variability on the ice sheet response timescales for the Tb_3 case where the melt rates and discharge are consistent with observed (supporting information S3; Adusumilli et al., 2020; Li et al., 2016). We aim to characterize the faster response timescales to ocean-driven ice shelf melt—due to changes in buttressing and grounding line migration—by investigating the correlation time offsets between ice shelf melting and discharge.

We analyze 2-month output time series from years 275 to 475 of the Tb_3 variable simulations, a period over which the grounding line location is relatively stable (i.e., perturbations generally <5 km over the 200-year period) and contact is maintained at the rumpled. The power spectra of ice discharge show higher power at lower frequencies for all variability amplitudes (Figure 3a), despite higher power at higher frequencies in the subsurface temperatures and melt rates (Figure S7).

The strongest agreement in the normalized power of the melt rates and discharge occurs on decadal to multidecadal timescales. We apply a lowpass filter with a 20-year cutoff to the melt rate and discharge time series, and cross-correlate these variables across a range of time lags (Figure 3b). The median lag time that maximizes the normalized cross-correlation corresponds with the ice discharge lagging the ocean-driven melt by 6 years (Figure 3c). Roberts et al. (2017) hypothesized that the rumpled play an important role in determining the ice sheet response timescales to ocean forcing. In their study, they reported a ~ 7 -year periodicity in surface elevation changes at the rumpled, which corresponds well with the estimate of the lag time between melt extrema and discharge found in our variability simulations and with variability in our TIS thickness record (Figure S8). Our results support the hypothesis that the rumpled play an important role in controlling the higher-frequency ice sheet response—grounding line stability and mass loss—under ocean forcing similar to present-day.

An increase in the variability amplitude leads to relatively higher power at higher frequencies of melt (Figure S7) and a shorter lag time between melt and discharge compared with VA1–VA3 (Figure 3). However, our VA1 simulation—in which the melt rate spectrum is dominated by low-frequency modes—still leads to lower discharge compared to the constant case, highlighting the importance of variability in modifying the ice sheet dynamic response.

Previous studies (Hoffman et al., 2019; Snow et al., 2017) show that low-frequency forcing modes (i.e., forcing on timescales greater than the ice shelf residence time) have a controlling influence on the ice sheet

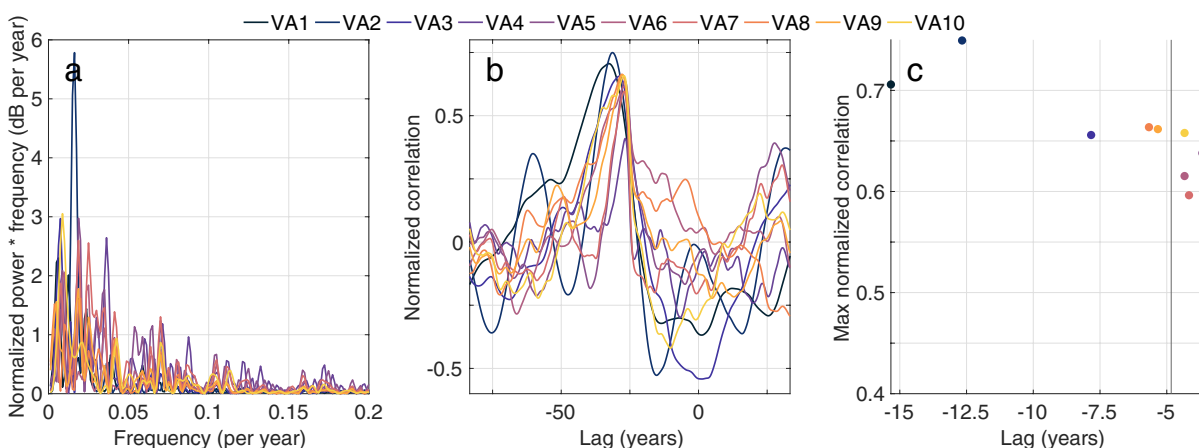


Figure 3. Analysis of the Tb_3 simulations VA1–VA10, for high resolution (2-month) output between years 275 and 475. (a) Lomb-Scargle power spectral density of discharge; (b) lead-lag cross-correlation between melt and discharge, where the autocorrelation of each time series at zero lag is normalized to be identically 1.0 and where a lowpass filter with a 20-year cutoff has been applied to the melt rate and discharge time series; (c) lag time (years) of maximum normalized correlation between melt and discharge (a negative lag indicates that melt leads discharge), where the vertical line represents the median lag time (−6 years) across the simulations.

response timescales. Recent work also shows that ocean forcing on decadal timescales can have centennial-scale impacts on the ice sheet response (Christian et al., 2020). Our ocean forcing contains relatively high power on decadal timescales (Figure S2b). However, the spectra of the resulting melt rates reflect intrinsic ice shelf-ocean interactions, and do not necessarily correlate with the forcing spectra or show dominance in the lower frequency modes. This may impact the consequent ice sheet response timescales in our simulations.

Furthermore, we did not consider the impact of specific, idealized periods of forcing on the ice sheet response, although it is inevitable that a change in the forcing spectrum (e.g., containing more quiescent periods, or more power at low frequencies) would lead to different results. Instead, our results show that small changes in the ocean variability amplitude can lead to large differences in the ice sheet response timescales and at spatial and temporal scales that require local observations to quantify. Changing the period could result in similarly large differences, particularly when these changes in thermal forcing trigger the crossing of thresholds or tipping points in the ice sheet response. Future work should focus on better understanding the character and impact of the ocean forcing periods in this region, through long-term ocean observation and numerical modeling studies.

5. Conclusions

We investigated the impact of variable ocean thermal forcing on Totten Glacier stability and dynamics. Our results show that the system is highly sensitive to small perturbations both in the mean ocean state and in the amplitude of variability. We find that the grounding line is stable for a limited range of background temperatures close to present-day forcing (i.e., -0.95°C to -0.75°C). Outside this limited range, large-scale grounding line advance or retreat occurs, and the addition of variable forcing in these scenarios can reduce discharge and grounding line migration compared with constant forcing. Small differences in the amplitude of variable forcing—and the frequencies that this can amplify or attenuate—under common background temperatures can lead to decadal-scale to centennial-scale delays in grounding line migration. This suggests that the forcing amplitude is not necessarily a clear predictor of the ice sheet response timescales.

Our results show that the degree to which ocean variability impacts ice dynamics, and the timescales over which the response occurs, depends on the complex interplay between the ocean mean state and variability, and ice sheet-topographic interactions. Further investigation into the complexities of the ice-climate interactions in this system is required to establish thresholds for future instability. This is particularly relevant given the lack of agreement in future scenarios of climate forcing (e.g., see Greene et al., 2017), and the fact that dominant modes of global climate variability show strong interdecadal and intercentennial

modulation (e.g., Wittenberg, 2009). Such an investigation should include: repeat (seasonal and multi-year) hydrographic measurements to characterize ocean variability and trends; characterization of tropical to polar atmospheric teleconnections that drive variability in the wind stress fields and consequent upwelling of CDW onto the continental shelf; more accurate and precise mapping of (potentially small-scale) topography, particularly near the southern end of the grounding line and in regions where the topography plays an important role in stabilizing the system; and model ensembles to investigate uncertainty in projections of future sea-level rise.

Data Availability Statement

All of the data sets and source code used in this study are publicly available. The authors use version 4.19 of the open-source ISSM software, which is freely available for download from <https://issm.jpl.nasa.gov/download/>. All the model initialization data sets used in this study are already available and are cited in this study and its supporting information file. The script used to parameterize the model is also provided as supporting information (ds01.par).

Acknowledgments

The authors thank two anonymous reviewers for their constructive comments that greatly improved the manuscript. This study was supported under the Australian Research Council's Special Research Initiative for Antarctic Gateway Partnership (Project ID SR140300001) and conducted by F. S. McCormack as part of a Fulbright Postdoctoral Award at the University of California, Irvine, USA. This study was undertaken with the assistance of resources from the Tasmanian Partnership for Advanced Computing and the National Computational Infrastructure, which is supported by the Australian Government.

References

- Adusumilli, S., Fricker, H. A., Medley, B., Padman, L., & Siegfried, M. R. (2020). Interannual variations in meltwater input to the Southern Ocean from Antarctic ice shelves. *Nature Geoscience*, 13(9), 616–620. <https://doi.org/10.1038/s41561-020-0616-z>
- Aitken, A. R. A., Roberts, J. L., Ommen, T. D. V., Young, D. A., Gollidge, N. R., Greenbaum, J. S., et al. (2016). Repeated large-scale retreat and advance of Totten Glacier indicated by inland bed erosion. *Nature*, 533, 385–389. <https://doi.org/10.1038/nature17447>
- Budd, W. F., Keage, P. L., & Blundy, N. A. (1979). Empirical studies of ice sliding. *Journal of Glaciology*, 23(89), 157–170. <https://doi.org/10.3189/S0022143000029804>
- Christian, J. E., Robel, A. A., Proistosescu, C., Roe, G., Koutnik, M., & Christianson, K. (2020). The contrasting response of outlet glaciers to interior and ocean forcing. *The Cryosphere*, 14, 2515–2535. <https://doi.org/10.5194/tc-14-2515-2020>
- Flament, T., & Rémy, F. (2012). Dynamic thinning of Antarctic glaciers from along-track repeat radar altimetry. *Journal of Glaciology*, 58(211), 830–840. <https://doi.org/10.3189/2012JoG11J118>
- Greenbaum, J. S., Blankenship, D. D., Young, D. A., Richter, T. G., Roberts, J. L., Aitken, A. R. A., et al. (2015). Ocean access to a cavity beneath Totten Glacier in East Antarctica. *Nature Geoscience*, 8, 294–298. <https://doi.org/10.1038/ngeo2388>
- Greene, C. A., Blankenship, D. D., Gwyther, D. E., Silvano, A., & van Wijk, E. (2017). Wind causes Totten Ice Shelf melt and acceleration. *Science Advances*, 3(11), e1701681. <https://doi.org/10.1126/sciadv.1701681>
- Gudmundsson, G. H., Paolo, F. S., Adusumilli, S., & Fricker, H. A. (2019). Instantaneous Antarctic ice sheet mass loss driven by thinning ice shelves. *Geophysical Research Letters*, 46(23), 13903–13909. <https://doi.org/10.1029/2019GL085027>
- Gwyther, D. E., O'Kane, T. J., Galton-Fenzi, B. K., Monselesan, D. P., & Greenbaum, J. S. (2018). Intrinsic processes drive variability in basal melting of the Totten Glacier Ice Shelf. *Nature Communications*, 9(1), 3141. <https://doi.org/10.1038/s41467-018-05618-2>
- Hoffman, M. J., Asay-Davis, X., Price, S. F., Fyke, J., & Perego, M. (2019). Effect of subshelf melt variability on sea level rise contribution from Thwaites Glacier, Antarctica. *Journal of Geophysical Research: Earth Surface*, 124(12), 2798–2822, e2019JF005155. <https://doi.org/10.1029/2019JF005155>
- Holland, P. R., Bracegirdle, T. J., Dutrieux, P., Jenkins, A., & Steig, E. J. (2019). West Antarctic ice loss influenced by internal climate variability and anthropogenic forcing. *Nature Geoscience*, 12, 718–724. <https://doi.org/10.1038/s41561-019-0420-9>
- Jacobs, S. S., Giulivi, C., Dutrieux, P., Rignot, E., Nitsche, F., & Mouginit, J. (2013). Getz Ice Shelf melting response to changes in ocean forcing. *Journal of Geophysical Research: Oceans*, 118(9), 4152–4168. <https://doi.org/10.1002/jgrc.20298>
- Jacobs, S. S., Hellmer, H. H., & Jenkins, A. (1996). Antarctic ice sheet melting in the Southeast Pacific. *Geophysical Research Letters*, 23(9), 957–960. <https://doi.org/10.1029/96GL00723>
- Jacobs, S. S., Jenkins, A., Giulivi, C. F., & Dutrieux, P. (2011). Stronger ocean circulation and increased melting under Pine Island Glacier ice shelf. *Nature Geoscience*, 4(8), 519–523. <https://doi.org/10.1038/Ngeo1188>
- Jenkins, A., Dutrieux, P., Jacobs, S. S., McPhail, S. D., Perrett, J. R., Webb, A. T., & White, D. (2010). Observations beneath Pine Island Glacier in West Antarctica and implications for its retreat. *Nature Geoscience*, 3, 468–472. <https://doi.org/10.1038/ngeo890>
- Jenkins, A., Shoosmith, D., Dutrieux, P., Jacobs, S., Kim, T. W., Lee, S. H., et al. (2018). West Antarctic Ice Sheet retreat in the Amundsen Sea driven by decadal oceanic variability. *Nature Geoscience*, 11(10), 733–738. <https://doi.org/10.1038/s41561-018-0207-4>
- Jezek, K. (2013). *RAMP AMM-1 SAR image mosaic of Antarctica, version 2*. <https://doi.org/10.5067/8AF4ZRPULS4H>
- Larour, E., Seroussi, H., Morlighem, M., & Rignot, E. (2012). Continental scale, high order, high spatial resolution, ice sheet modeling using the Ice Sheet System Model (ISSM). *Journal of Geophysical Research*, 117(F01022). <https://doi.org/10.1029/2011JF002140>
- Lazeroms, W. M. J., Jenkins, A., Gudmundsson, G. H., & van de Wal, R. S. W. (2018). Modelling present-day basal melt rates for Antarctic ice shelves using a parametrization of buoyant meltwater plumes. *The Cryosphere*, 12, 49–70. <https://doi.org/10.5194/tc-12-49-2018>
- Lenaerts, J. T. M., van den Broeke, M. R., van de Berg, W. J., van Meijgaard, E., & Kuipers Munneke, P. (2012). A new, high-resolution surface mass balance map of Antarctica (1979–2010) based on regional atmospheric climate modeling. *Geophysical Research Letters*, 39. <https://doi.org/10.1029/2011GL050713>
- Li, X., Rignot, E., Mouginit, J., & Scheuchl, B. (2016). Ice flow dynamics and mass loss of Totten Glacier, East Antarctica, from 1989 to 2015. *Geophysical Research Letters*, 43(12), 6366–6373. <https://doi.org/10.1002/2016GL069173>
- MacAyeal, D. R. (1989). Large-scale ice flow over a viscous basal sediment: Theory and application to Ice Stream B, Antarctica. *Journal of Geophysical Research: Solid Earth*, 94(B4), 4071–4087. <https://doi.org/10.1029/jb094ib04p04071>
- Morlighem, M., Rignot, E., Binder, T., Blankenship, D., Drews, R., Eagles, G., et al. (2020). Deep glacial troughs and stabilizing ridges unveiled beneath the margins of the Antarctic ice sheet. *Nature Geoscience*, 13, 132–137. <https://doi.org/10.1038/s41561-019-0510-8>

- Morlighem, M., Seroussi, H., Larour, E., & Rignot, E. (2013). Inversion of basal friction in Antarctica using exact and incomplete adjoints of a higher-order model. *Journal of Geophysical Research: Earth Surface*, 118(3), 1746–1753. <https://doi.org/10.1002/jgrf.20125>
- Nitsche, F. O., Porter, D., Williams, G., Cougnon, E. A., Fraser, A. D., Correia, R., & Guerrero, R. (2017). Bathymetric control of warm ocean water access along the East Antarctic Margin. *Geophysical Research Letters*, 44(17), 8936–8944. <https://doi.org/10.1002/2017GL074433>
- Oppenheimer, M., Glavovic, B. C., Hinkel, J., van de Wal, R., Magnan, A. K., Abd-Elgawad, A., & Pereira, J. (2019). Sea level rise and implications for low-lying islands, coasts and communities. In *IPCC special report on the ocean and cryosphere in a changing climate* (p. 126). Paolo, F. S., Fricker, H. A., & Padman, L. (2015). Volume loss from Antarctic ice shelves is accelerating. *Science*, 348, 327–331. <https://doi.org/10.1126/science.aaa0940>
- Pelle, T., Morlighem, M., & Bondzio, J. H. (2019). Brief communication: PICOP, a new ocean melt parameterization under ice shelves combining PICO and a plume model. *The Cryosphere*, 13(3), 1043–1049. <https://doi.org/10.5194/tc-13-1043-2019>
- Pelle, T., Morlighem, M., & McCormack, F. S. (2020). Aurora Basin, the weak underbelly of East Antarctica. *Geophysical Research Letters*, 47(9), e2019GL086821. <https://doi.org/10.1029/2019GL086821>
- Reese, R., Albrecht, T., Mengel, M., Asay-Davis, X., & Winkelmann, R. (2018). Antarctic sub-shelf melt rates via PICO. *The Cryosphere*, 12, 1969–1985. <https://doi.org/10.5194/tc-12-1969-2018>
- Rignot, E., Mouginot, J., & Scheuchl, B. (2011). Ice flow of the Antarctic Ice Sheet. *Science*, 333(6048), 1427–1430. <https://doi.org/10.1126/science.1208336>
- Rignot, E., Mouginot, J., & Scheuchl, B. (2017). *MEaSURES InSAR-based Antarctica ice velocity map 450m Version 2.0*. NASA National Snow and Ice Data Center Distributed Active Archive Center. <https://doi.org/10.5067/D7GK8F5J8M8R>
- Rintoul, S. R., Silvano, A., Pena-Molino, B., van Wijk, E., Rosenberg, M., Greenbaum, J. S., & Blankenship, D. D. (2016). Ocean heat drives rapid basal melt of the Totten Ice Shelf. *Science Advances*, 2(12), e1601610. <https://doi.org/10.1126/sciadv.1601610>
- Robel, A. A., Seroussi, H., & Roe, G. H. (2019). Marine ice sheet instability amplifies and skews uncertainty in projections of future sea-level rise. *Proceedings of the National Academy of Sciences of the United States of America*, 116(30), 14887–14892. <https://doi.org/10.1073/pnas.1904822116>
- Roberts, J., Galton-Fenzi, B. K., Paolo, F. S., Donnelly, C., Gwyther, D. E., Padman, L., et al. (2017). Ocean forced variability of Totten Glacier mass loss. *Geological Society London Special Publications*, 461, 175–186. <https://doi.org/10.1144/SP461.6>
- Schlegel, N.-J., Seroussi, H., Schodlok, M. P., Larour, E. Y., Boening, C., Limonadi, D., et al. (2018). Exploration of Antarctic Ice Sheet 100-year contribution to sea level rise and associated model uncertainties using the ISSM framework. *The Cryosphere*, 12(11), 3511–3534. <https://doi.org/10.5194/tc-12-3511-2018>
- Schmidtke, S., Heywood, K. J., Thompson, A. F., & Aoki, S. (2014). Multidecadal warming of Antarctic waters. *Science*, 346(6214), 1227–1231. <https://doi.org/10.1126/science.1256117>
- Schoof, C. (2007). Ice sheet grounding line dynamics: Steady states, stability, and hysteresis. *Journal of Geophysical Research*, 112(F03S28), 1–19. <https://doi.org/10.1029/2006JF000664>
- Seroussi, H., & Morlighem, M. (2018). Representation of basal melting at the grounding line in ice flow models. *The Cryosphere*, 12(10), 3085–3096. <https://doi.org/10.5194/tc-12-3085-2018>
- Seroussi, H., Nakayama, Y., Larour, E., Menemenlis, D., Morlighem, M., Rignot, E., & Khazendar, A. (2017). Continued retreat of Thwaites Glacier, West Antarctica, controlled by bed topography and ocean circulation. *Geophysical Research Letters*, 44, 6191–6199. <https://doi.org/10.1002/2017GL072910>
- Seroussi, H., Nowicki, S., Payne, A. J., Goelzer, H., Lipscomb, W. H., Abe Ouchi, A., & Zwinger, T. (2020). ISMIP6 Antarctica: A multi-model ensemble of the Antarctic ice sheet evolution over the 21st century. *The Cryosphere*, 14, 3033–3070. <https://doi.org/10.5194/tc-14-3033-2020>
- Silvano, A., Rintoul, S. R., Peña-Molino, B., & Williams, G. D. (2017). Distribution of water masses and meltwater on the continental shelf near the Totten and Moscow University ice shelves. *Journal of Geophysical Research: Oceans*, 122(3), 2050–2068. <https://doi.org/10.1002/2016JC012115>
- Smith, B., Fricker, H. A., Gardner, A. S., Medley, B., Nilsson, J., Paolo, F. S., et al. (2020). Pervasive ice sheet mass loss reflects competing ocean and atmosphere processes. *Science*, 368(6496), 1239–1242. <https://doi.org/10.1126/science.aaz5845>
- Snow, K., Goldberg, D. N., Holland, P. R., Jordan, J. R., Arthern, R. J., & Jenkins, A. (2017). The response of ice sheets to climate variability. *Geophysical Research Letters*, 44, 878–911. <https://doi.org/10.1002/2017GL075745>
- Storch, H. V., & Zwiers, F. W. (1999). *Statistical analysis in climate research*. Cambridge University Press. <https://doi.org/10.1017/CBO9780511612336>
- Sun, S., Cornford, S. L., Gwyther, D. E., Gladstone, R. M., Galton-Fenzi, B. K., Zhao, L., & Moore, J. C. (2016). Impact of ocean forcing on the Aurora Basin in the 21st and 22nd centuries. *Annals of Glaciology*, 57(73), 79–86. <https://doi.org/10.1017/aog.2016.27>
- Wakatsuchi, M., Ohshima, K. I., Hishida, M., & Naganobu, M. (1994). Observations of a street of cyclonic eddies in the Indian Ocean sector of the Antarctic Divergence. *Journal of Geophysical Research*, 99(C10), 20417–20426. <https://doi.org/10.1029/94JC01478>
- Weertman, J. (1974). Stability of the junction of an ice sheet and an ice shelf. *Journal of Glaciology*, 13(67), 3–11. <https://doi.org/10.3189/S0022143000023327>
- Williams, G. D., Meijers, A. J. S., Poole, A., Mathiot, P., Tamura, T., & Klocker, A. (2011). Late winter oceanography off the Sabrina and Banzare coast (117–128°E), East Antarctica. *Deep Sea Research Part II: Topical Studies in Oceanography*, 58(9), 1194–1210. <https://doi.org/10.1016/j.dsr2.2010.10.035>
- Wittenberg, A. T. (2009). Are historical records sufficient to constrain ENSO simulations? *Geophysical Research Letters*, 36(12). <https://doi.org/10.1029/2009GL038710>
- Yu, H., Rignot, E., Seroussi, H., & Morlighem, M. (2018). Retreat of Thwaites Glacier, West Antarctica, over the next 100 years using various ice flow models, ice shelf melt scenarios and basal friction laws. *The Cryosphere*, 12(12), 3861–3876. <https://doi.org/10.5194/tc-12-3861-2018>

References From the Supporting Information

- Brondex, J., Gillet-Chaulet, F., & Gagliardini, O. (2019). Sensitivity of centennial mass loss projections of the Amundsen basin to the friction law. *The Cryosphere*, 13(1), 177–195. <https://doi.org/10.5194/tc-13-177-2019>
- Galton-Fenzi, B. K., Hunter, J. R., Coleman, R., Marsland, S. J., & Warner, R. C. (2012). Modeling the basal melting and marine ice accretion of the Amery Ice Shelf. *Journal of Geophysical Research*, 117(C9). <https://doi.org/10.1029/2012JC008214>

- Glen, J. W. (1955). The creep of polycrystalline ice. *Proceedings of the Royal Society A*, 228(1175), 519–538. <https://doi.org/10.1098/rspa.1955.0066>
- Gwyther, D. E., Galton-Fenzi, B. K., Hunter, J. R., & Roberts, J. L. (2014). Simulated melt rates for the Totten and Dalton ice shelves. *Ocean Science*, 10(3), 267–279. <https://doi.org/10.5194/os-10-267-2014>
- Hansen, P. C. (2000). The L-curve and its use in the numerical treatment of inverse problems. In P. Johnston, (Ed.), *Computational inverse problems in electrocardiology. Advances in Computational Bioengineering* (pp. 119–142). WIT Press.
- Joughin, I., Smith, B. E., & Schoof, C. G. (2019). Regularized Coulomb friction laws for ice sheet sliding: Application to Pine Island Glacier, Antarctica. *Geophysical Research Letters*, 46(9), 4764–4771. <https://doi.org/10.1029/2019GL082526>
- Large, W., & Yeager, S. (2004). *Diurnal to decadal global forcing for ocean and sea-ice models: The data sets and flux climatologies* (Tech. Rep.). UCAR/NCAR. <https://doi.org/10.5065/D6KK98Q6>
- Schoof, C. (2005). The effect of cavitation on glacier sliding. *Proceedings of the Royal Society A*, 461(2055), 609–627. <https://doi.org/10.1098/rspa.2004.1350>
- Seroussi, H., Morlighem, M., Larour, E., Rignot, E., & Khazendar, A. (2014). Hydrostatic grounding line parameterization in ice sheet models. *The Cryosphere*, 8(6), 2075–2087. <https://doi.org/10.5194/tc-8-2075-2014>
- Shchepetkin, A., & McWilliams, J. C. (2005). The regional oceanic modeling system (ROMS): A split-explicit, free-surface, topography-following-coordinate oceanic model. *Ocean Modelling*, 9, 347–404.
- Tamura, T., Williams, G. D., Fraser, A. D., & Ohshima, K. I. (2012). Potential regime shift in decreased sea ice production after the Mertz Glacier calving. *Nature Communications*, 3(1), 826. <https://doi.org/10.1038/ncomms1820>
- Tsai, V., Stewart, A., & Thompson, A. (2015). Marine ice-sheet profiles and stability under Coulomb basal conditions. *Journal of Glaciology*, 61(226), 205–215. <https://doi.org/10.3189/2015JoG14J221>
- Weertman, J. (1957). Deformation of floating ice shelves. *Journal of Glaciology*, 3(21), 38–42. <https://doi.org/10.3189/S0022143000024710>